

Ultra-Wideband Six-port Network Constructed by 90° and In-Phase Power Dividers

Norhudah Seman^{1*}, Khairul Huda Yusof², Mohd Haizal Jamaluddin¹,
and Tharek Abd Rahman¹

¹Wireless Communication Centre, School of Electrical Engineering
University Teknologi Malaysia, 81310 UTM Johor Bahru, Johor, Malaysia
huda@fke.utm.my, haizal@fke.utm.my, tharek@fke.utm.my

²Faculty of Engineering and Information Technology, MAHSA University, 42610 Jenjarom, Selangor, Malaysia
khairulhuda@mahsa.edu.my

Abstract — This article proposes a six-port network design with an ultra-wideband operation from 3.1 to 10.6 GHz. The proposed six-port configuration is constructed by two types of power dividers with different phase characteristics of 0° (in-phase) and 90°. The new proposed configuration eliminates one unused port of the conventional six-port. Both components forming the proposed six-port are designed utilizing the microstrip-slot technique to accomplish the designated UWB operating frequency. The six-port is designed via the use of CST Microwave Studio (CST MWS) and realised by applying Rogers TMM4 substrate. Comparable simulated and measured performances are achieved in terms of S-parameters and phase differences between each consecutive port across UWB frequency range.

Index Terms — Microstrip-slot, power divider, six-port, ultra-wideband.

I. INTRODUCTION

Nowadays, an intense growth in the number of mobile broadband service subscribers is noted every year. There is an increasing demand for mobile and faster Internet access, instant communication with others, immediate access to information and advanced multimedia, and latest trendy wireless mobile devices such as smartphones and tablets. Hence, the designers and engineers are facing endlessly requirement of new wireless devices and applications for mobility and high data rate. Attributable to the demand, the fifth-generation (5G) wireless system that anticipated being deployed by 2020 is extensively studied. 5G will realise network capability of providing zero-distance connectivity between people and connected machines. The architecture of new 5G technologies has a separated solution for the applications in indoor and outdoor. Particularly for applications in indoor, the architecture applies a

distributed antenna system (DAS) solution, while for outdoor, massive multiple-input multiple-output (MIMO) technology is utilized [1]. Therefore, high-data-rate and high-quality services to indoor users can be offered, whilst simultaneously lessening the pressure on outdoor applications. In order to fulfill this necessity, numerous researches are conducted in the designs of front-end components such as a complementary option to the mixer. Commonly, the mixer design utilizes active devices that require a biasing circuit that causes design complexity. This mixer-based approach in the front-end communication transceiver can be replaced by using a six-port network to reduce the complexity. Similar to the mixer, six-port can operate as a modulator and demodulator [2]-[4]. This alternative architecture of the six-port network does not require any use of active devices, which eliminates the existence of intermediate frequency (IF) and the image produced by the mixer. Consequently, the high price-tag IF filter and image rejection filter are not required in the design [5]. Therefore, with the use of the six-port network in the transceiver system, the complexity of the circuit can be reduced and allows easier circuit integration with other components.

Various design techniques have been studied to realise a wideband six-port. Such as in [6], a compact six-port design is proposed, which comprises four 90° hybrid rounded couplers. This six-port has a bandwidth of 570 MHz, which operates from 1.68 to 2.25 GHz. The design is realised using Rogers 3006 substrate with a size of 65 x 65 mm². A smaller size of a six-port network is proposed in [7] with a 55 x 61 mm² that composed by one Wilkinson power divider and three miniaturized 90° hybrid couplers. In the proposed design, four transmission lines, which utilizes two high-low impedance shunt stubs have been introduced to the designed power divider and 90° hybrid coupler in order to reduce six-port size. It has

a fairly good performance across a frequency band of 2.2-2.6 GHz, which narrower than [6]. Meanwhile in [8], another design of six-port network for a reflection coefficient measurement purpose has been reported, which contains a Wilkinson power divider, four coupled-line couplers and a section of a transmission line. Its performance is experimentally verified across a frequency range of 2-3.5 GHz.

However, the six-port networks proposed in [4]-[8] have limited bandwidth, which may be inapplicable in applications that require a wider band. Thus, considering this bandwidth limitation, a wideband six-port network is proposed by Ibrahim et. al in [9] by integrating four quadrature and in-phase Wilkinson dividers. In this proposed design, the quadrature Wilkinson divider has a phase difference of 90° between its two output ports, which obtained through the implementation of a 90° phase shifter at one of the output ports. Furthermore, the configuration used in this design has eliminated one unused port that contributes to lessening error. Despite that, its performance only covers from 3 to 8 GHz. As known, the more components used, the more transmission lines are required that leads to higher losses as the signals have to go through many transmission lines. Another technique to increase bandwidth is by using the multilayer technique [2]. In [2], the proposed six-port is constructed by using three tight coupling rectangular-shaped couplers with virtual stubs and an in-phase power divider with equal power division. Multilayer microstrip-slot design technique is used in the proposed six-port to enhance the operating frequency. It has demonstrated agreeable simulated and measured across 2-6 GHz with small dimension size of 54 mm x 62 mm. The use of two substrates in this multilayer structure of six-port may lead to difficulty in fabrication, which experiencing problems of an air gap and misalignment. Even though the performances proposed in [2] and [9] are wider, but still not covering the desired UWB frequency range.

Thus, to overcome the problems in [2], [4]-[9], a new six-port network design that can operate over the UWB frequency range is essential to be proposed. Each of the components constituting the proposed six-port is designed by implementing the microstrip-slot technique. The design applies Rogers TMM4 substrate that has 4.5 relative permittivity, 0.002 loss tangent, 35 μm conductor coating and 0.508 mm substrate thickness.

II. SIX-PORT NETWORK DESIGN

The new design six-port network is having a configuration that integrates three in-phase power dividers (D), which two of them are connected to three 90° power dividers (90° D) as presented in Fig. 1. Moreover, it can be noted from Fig. 1, the input ports of the six-port network are labeled as P1 and P2, meanwhile the output ports as P3, P4, P5 and P6. This new configuration eliminates one unused port of conventional six-port

configuration that requires matched termination as presented in [2], [3] and [7].

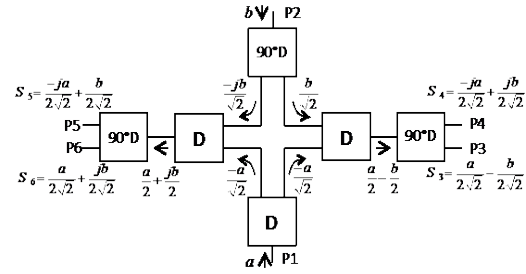


Fig. 1. The block diagram of the proposed six-port configuration.

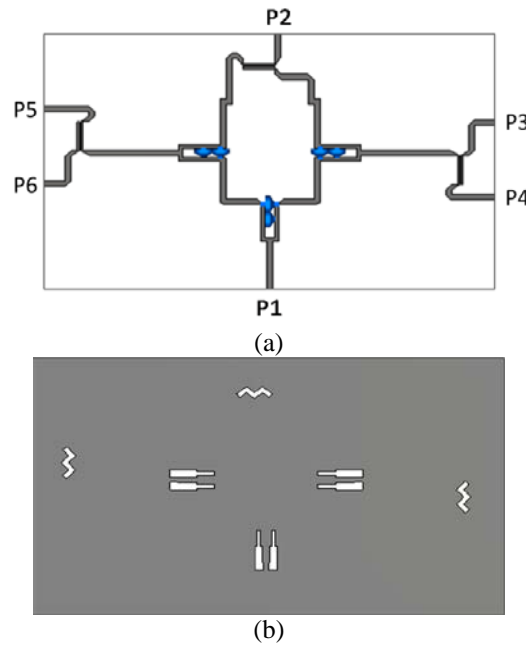


Fig. 2. The layout view of (a) top and (b) bottom layer of the proposed six-port network.

As presented by the configuration in Fig. 1, the proposed six-port has four output signals at its respective output ports of P3 to P6, which are denoted as S_i . i are referring to the output ports, which can be derived as follows:

$$S_3 = \frac{a}{2\sqrt{2}} - \frac{b}{2\sqrt{2}}, \quad (1)$$

$$S_4 = -j\frac{a}{2\sqrt{2}} + j\frac{b}{2\sqrt{2}}, \quad (2)$$

$$S_5 = -j\frac{a}{2\sqrt{2}} + \frac{b}{2\sqrt{2}}, \quad (3)$$

$$S_6 = \frac{a}{2\sqrt{2}} + j\frac{b}{2\sqrt{2}}, \quad (4)$$

where the input signals are denoted by the variable a

and b at the respective Port 1 (P1) and Port 2 (P2). Meanwhile, the symbol of ‘ j ’ implies a phase shift or delay by 90° of the complex signal. The design and simulation of the UWB six-port network are concerning the centre frequency of 6.85 GHz with a designated range of 3.1-10.6 GHz, which performed by employing CST Microwave Studio (CST MWS). The CST MWS generated layout of the proposed six-port network is presented in Fig. 2.

A. In-phase power divider (D)

The layout of the power divider with equal power division and 0° phase difference (in-phase) between its output ports that used in the construction of the six-port network and its fabricated prototype are depicted in the respective Figs. 3 and 4. The design comprises of the top conductive layer, which has microstrip lines that linked to three designated ports of Ports 1 to 3 (P1 – P3). Whilst at the ground plane, there are two rectangular-shaped slots that placed symmetrically beneath microstrip lines of output arms. The transmission line of microstrip with a slot underneath is also branded by term ‘microstrip-slot’ [10]. These microstrip-slot lines with the characteristic impedance of Z_1 (84.09 ohm) and Z_2 (59.46 ohm) form two-section quarter-wave transformers to achieve the bandwidth specification. Two resistors, R_1 (130 ohm) and R_2 (200 ohm) are positioned at the end of each quarter-wave transformer section to ensure good isolation is achieved between output ports, and any reflected power is dissipated at wider frequency range.

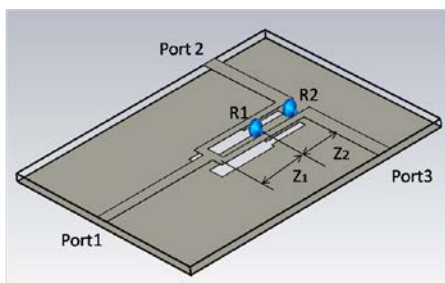


Fig. 3. The in-phase power divider layout in its perspective view.

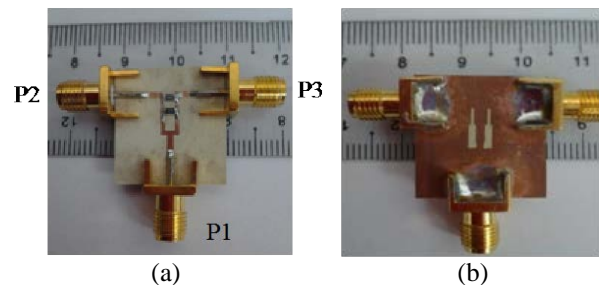


Fig. 4. (a) Top and (b) bottom view of the fabricated power divider.

This two-section power divider has a UWB operation within 3.1 to 10.6 GHz demonstrated by the presented results of simulation and measurement in Fig. 5. As demonstrated in Fig. 5 (a), it is noted that the results of S_{21} and S_{31} for simulation and measurement are showing an almost similar performance of -3.55 ± 0.15 dB and -3.8 ± 0.5 dB across 3 to 11 GHz, accordingly. Meanwhile, the simulation and measurement results of S_{11} and S_{23} are less than -10 dB. Furthermore, the simulation result for the phase characteristic is $0^\circ \pm 0.2^\circ$ between Ports 2 and 3 as shown in Fig. 5 (b). While the measurement result is showing a comparable performance with a slight degradation of $0^\circ \pm 2^\circ$ across 3.1 to 10.6 GHz. This observed degradation could be due to the small difference in transmission lines’ lengths of the fabricated prototype compared the simulated design, which occurred normally.

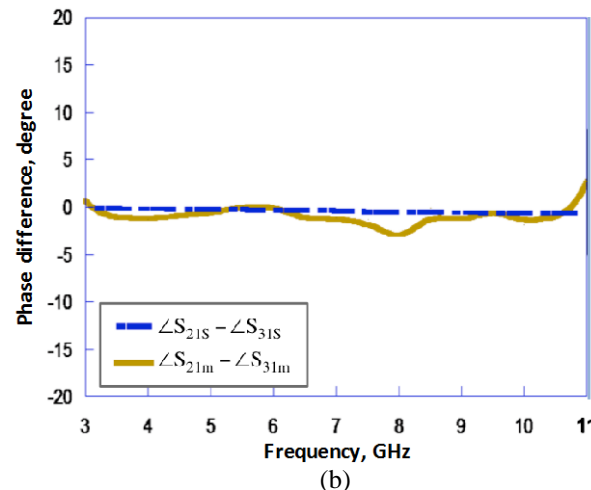
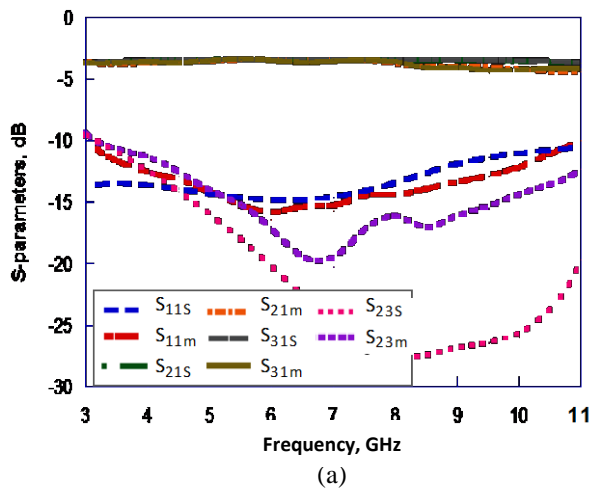


Fig. 5. The performance of (a) S-parameter characteristics and (b) phase difference between Ports 2 and 3 of the power divider (notation ‘s’ and ‘m’ are referring to the respective simulation and measurement).

By implementing the rectangular-shaped slot underneath microstrip line to construct the quarter-wave transformer into the design of the power divider, the quarter-wave transformer length can be reduced to 4.153 mm, which equivalent to $\lambda_{m-s}/4$ [10]. This is due to the deflection in the ground layer, which interrupts the current distribution. Subsequently, increase the effective inductance and capacitance of the microstrip line [11-12]. This contributes to reducing the size of the power divider circuit up to 23.33%. In addition to that, the bandwidth performance has been improved up to 11.9% compared to the conventional two-section power divider as described in [13]. Furthermore, it can be noted that it exhibits a good relative agreement between simulation and measurement result, which guarantee a wideband operation of the proposed six-port network.

B. 90° power divider (90° D)

Figures 6 and 7 illustrate the respective layout and prototype of the 90° power divider that used to form the proposed six-port network, that is attained via the removal of the coupled-line coupler's isolated port, which proposed in [14]. This design comprises of a microstrip coupled-line with a zig-zag-shaped slotline beneath that has an effective quarter-wavelength. Therefore, this divider has an equal power division and the phase difference of 90° between its output ports. The implementation of the zig-zag slot provides a slower phase velocity, which increases the length of the current path, that consequently reduces the total physical length of the divider [14-15].

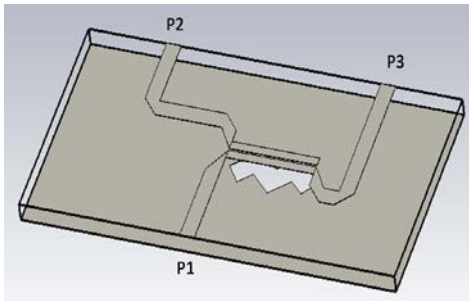


Fig. 6. The layout of the 90° power divider in its perspective view.

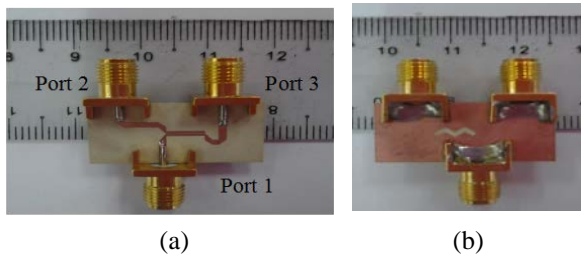
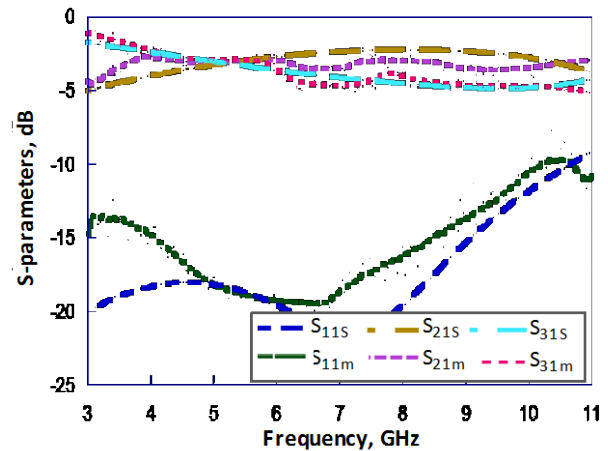
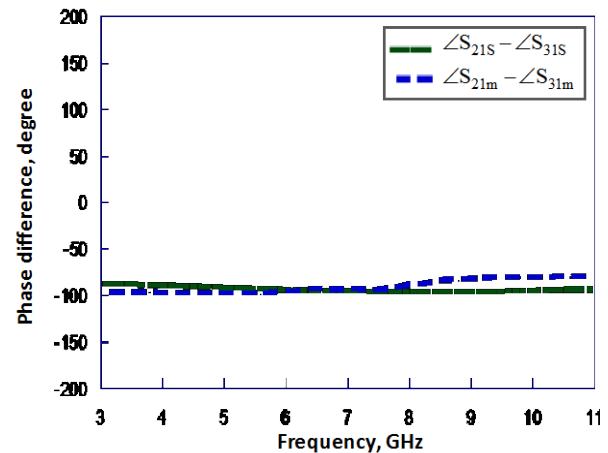


Fig. 7. The fabricated 90° power divider: (a) top and (b) bottom view.

As shown in Fig. 8, the divider operates well at UWB frequency range, verified by both simulation and measurement results. The simulated and measured S_{11} and S_{41} are less than -10 dB across 3.1 to 10.6 GHz. Whilst, both transmission coefficient results of S_{21} and S_{31} are approximately at -3 dB. In addition, Fig. 8 (b) shows the phase characteristic performance of the 90° power divider, where, both simulated and measured phase differences are $-90^\circ \pm 5^\circ$. Thus, a comparable simulation and measurement results can be observed. Therefore, this divider with very well UWB performance suits to be applied in the proposed six-port formation, which has the configuration as shown in Fig. 1.



(a)



(b)

Fig. 8. The simulated and measured (a) S-parameters and (b) phase characteristic of the 90° power divider (notation 's' and 'm' are referring to the respective simulation and measurement).

III. THE FABRICATED SIX-PORT NETWORK AND ITS PERFORMANCE

The fabricated of the proposed UWB six-port network forming by in-phase power dividers and 90°

power dividers is presented in Fig. 9. The proposed six-port is fabricated onto Rogers TMM4 substrate with 4.5 mm relative permittivity, 0.002 loss tangent, 35 μm conductor coating and 0.508 mm substrate thickness. This six-port network has a dimensional size of 81.7 x 50.92 mm².

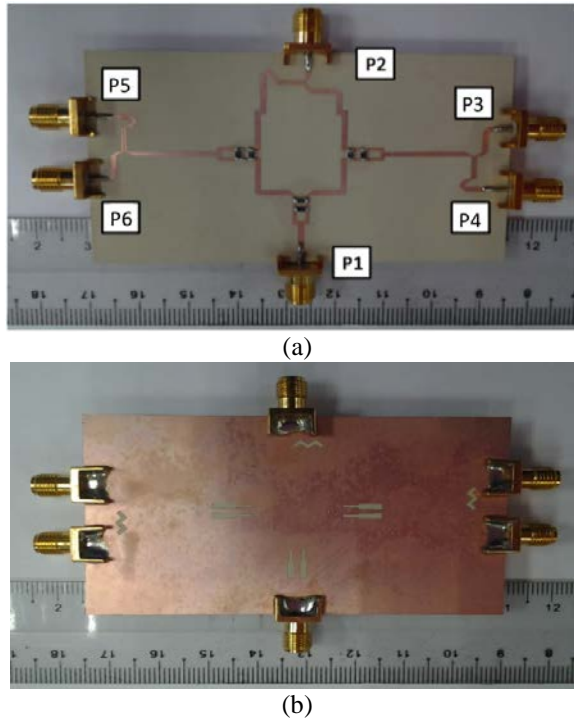


Fig. 9. The fabricated UWB six-port network: (a) top and (b) bottom view.

Figure 10 shows the simulation and measurement performance of the proposed six-port network. Both simulation and measurement performance are assessed considering S-parameters and phase differences between each consecutive port. First, the performance of transmission coefficients, S_{ij} , where $i = 3, 4, 5, 6$ and $j = 1, 2$ are evaluated. The simulated transmission coefficients of S_{i1} have the performance of $-9 \text{ dB} \pm 3 \text{ dB}$ within 3.1 and 10.6 GHz. While, the measured transmission coefficients of S_{i1} show a comparable performance of $-9 \text{ dB} \pm 4 \text{ dB}$, except S_{41} with $-13.5 \text{ dB} \pm 2.5 \text{ dB}$. Meanwhile, the simulated and transmission coefficients of S_{i2} perform the respective $-11 \text{ dB} \pm 4 \text{ dB}$, and $-13.5 \text{ dB} \pm 3 \text{ dB}$ from 3.1 to 10.6 GHz. The shown deviation is expected to be observed from the ideal value of -9 dB ($|S_{i1}| = |S_{i2}| = \frac{1}{2\sqrt{2}}$), which contributed from the individual imperfect performance of the in-phase power divider and 90° power divider. Furthermore, the microstrip lines used to connect the components are also contributing to the losses that lead to the observed deviation.

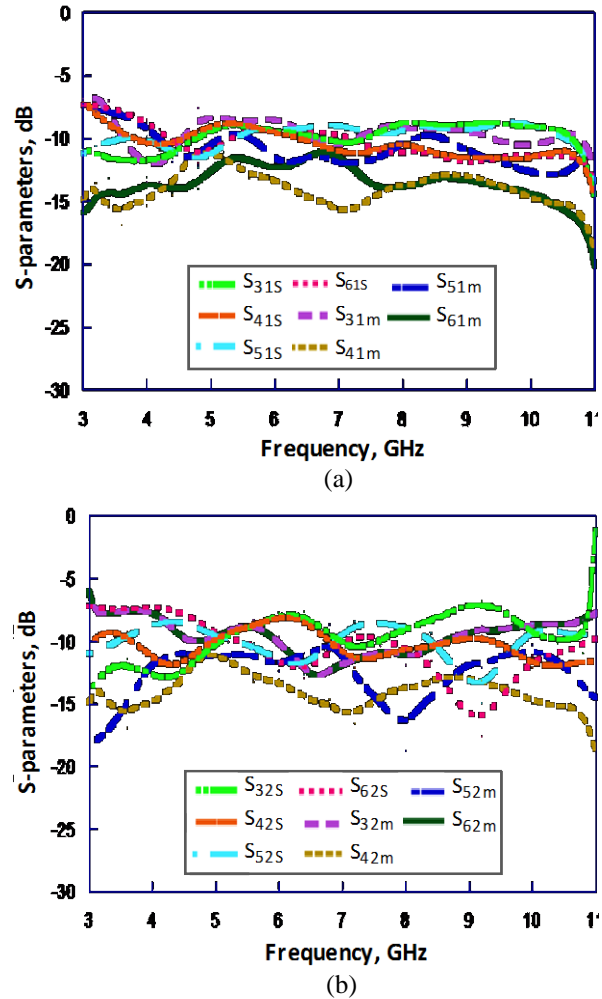


Fig. 10. The S-parameter performance of proposed six-port network: (a) transmission coefficients of S_{i1} , and (b) transmission coefficients of S_{i2} (notation ‘s’ and ‘m’ are referring to the respective simulation and measurement).

Then, the next concern is to evaluate the simulated and measured the performance of return loss at Port 1 and Port 2. From the observation, both demonstrate quite similar performances that exceed 10 dB across 3.1 to 10.6 GHz, as plotted in Fig. 11. Meanwhile, the simulation and measurement performance of isolation between Ports 1 and 2 also have comparable performance, where both are greater than 10 dB across the similar frequency range of UWB.

The next assessment concerns the simulation and measurement of the six-port network’s phase differences, which plotted in Fig. 12. The simulated and measured phase differences between Ports 3 and 4 are approximately at $90^\circ \pm 13^\circ$ and $90^\circ \pm 17^\circ$ over the designated operating frequency of 3.1–10.6 GHz, accordingly. While similar simulated and measured deviations of the respective $\pm 13^\circ$ and $\pm 17^\circ$ are noted from the ideal phase difference

between Port 5 and Port 6 of -90° .

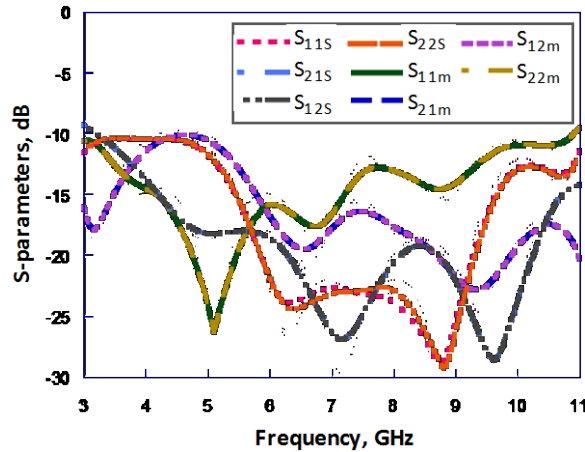


Fig. 11. The reflection coefficient and isolation performance of proposed six-port network (notation 's' and 'm' are referring to the respective simulation and measurement).

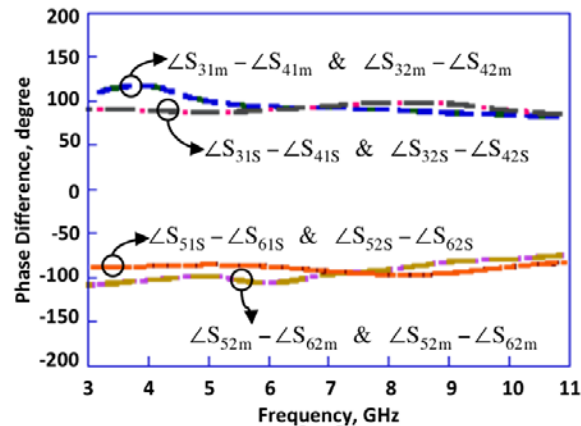


Fig. 12. The reflection coefficient and isolation performance of proposed six-port network (notation 's' and 'm' are referring to the respective simulation and measurement).

IV. CONCLUSION

This article has proposed a six-port network design with a capability of ultra-wideband (UWB) operation. The new proposed configuration of the six-port network is constructed by six 3-dB power dividers; three 90° dividers and three 0° (in-phase) dividers, which has been presented utilizing electromagnetic (EM) simulator of CST MWS. This configuration has removed one unused port in the conventional six-port configuration reported in [2] and [7]. Moreover, this six-port has accomplished a good UWB performance between simulation and measurement within operating frequency of 3.1 and 10.6 GHz with $81.7 \times 50.92 \text{ mm}^2$ overall dimensional size. Consequently, it has the best phase characteristic with the measured phase imbalance of $\pm 17^\circ$ compared

to the designs reported in [2] and [9], which are $\pm 29^\circ$, and $\pm 25^\circ$, accordingly. The bandwidth performance of proposed six-port has been increased up to 50% and 87.5% compared to the respective design in [9] and [2]. This improvement has been achieved due to the use of microstrip-slot in the design of individual components forming the six-port, which are 90° dividers and in-phase two-section power dividers.

ACKNOWLEDGMENT

This work is carried out with the financial support from the Malaysian Ministry of Education (MOE) and Universiti Teknologi Malaysia (UTM) via GUP, Flagship, HiCoE, PRGS and FRGS Grant with the respective vote number of 05H43, 03G41, 4J212, 4L684 and 5F048.

REFERENCES

- [1] C.-X. Wang, F. Haider, X. Gao, et al., "Cellular architecture and key technologies for 5G wireless communication networks," *IEEE Commun. Mag.*, vol. 52, no. 2, pp. 122-130, Feb. 2014.
- [2] N. Seman and S. N. A. M. Ghazali, "Quadrature phase shift keying (QPSK) modulator design using multi-port network in multilayer microstrip-slot technology for wireless communication applications," *Radioengineering*, vol. 24, no. 2, pp. 527-534, June 2015.
- [3] N. Seman and M. E. Bialkowski, "Design of a UWB microwave reflectometer with the use of a microstrip-slot technique," *Microw. Opt. Technol. Lett.*, vol. 51, no. 9, pp. 2169-2175, June 2009.
- [4] S. O. Tatu, E. Moldovan, K. Wu, and R. G. Bosisio, "A new direct millimeter-wave six-port receiver," *IEEE Trans. Microw. Theory Tech.*, vol. 49 no. 12, pp. 2517-2522, May 2001.
- [5] H.-S. Lim, W.-K. Kim, J.-W. Yo, H.-C. Park, W.-J. Byun, and M.-S. Song, "Compact six-port transceiver for time-division duplex system," *IEEE Microw. Wirel. Compon. Lett.*, vol. 17, no. 5, pp. 2766-2772, May 2007.
- [6] R. Hussain and M. S. Sharawi, "A dual six-port with two-angle resolution and compact size for mobile terminals," *IEEE Radio and Wireless Symp.*, Long Beach, CA, pp. 226-228, Jan. 2014.
- [7] X.-T. Fang, X.-C. Zhang, and C.-M. Tong, "A novel miniaturized microstrip six-port junction," *Progress In Electromagnetics Research Letters*, vol. 23, pp. 129-135, 2011.
- [8] K. Staszek, S. Gruszczynski, and K. Wincza, "Design and accuracy analysis of a broadband six-port reflectometer utilizing coupled line directional couplers," *Microw. Opt. Technol. Lett.*, vol. 55, no. 7, pp. 1485-1490, July 2013.
- [9] S. Z. Ibrahim, A. Abbosh, and M. Bialkowski, "Design of wideband six-port network formed by in-phase and quadrature Wilkinson dividers," *IET*

Microw. Antennas Propag., vol. 6, no. 11, pp. 1215-1220, Aug. 2012.

- [10] K. H. Yusof, N. Seman, M. H. Jamaluddin, and D. N. A. Zaidel, "Characterization and formulation of microstrip-slot impedance with different thickness and relative permittivity," *Applied Mechanics and Materials*, vol. 781, pp. 53-56, 2015.
- [11] A. S. Mohra, M. A. Alkanhal, and E. A. Abdullah, "Size-reduced defected ground microstrip directional coupler," *Microw. Opt. Technol. Lett.*, vol. 52, no. 9, pp. 1933-1937, Sep. 2010.
- [12] L. G. Maloratsky, "Microstrip circuit with a modified ground plane," *High Frequency Electronic, Summit Technical Media*, 2009.
- [13] L. G. Maloratsky, *Passive RF and Microwave Integrated Circuits*. Elsevier, 2004.
- [14] K. H. Yusof, N. Seman, M. H. Jamaluddin, and D. N. A. Zaidel, "Design of ultra wideband 3 dB coupled-line coupler and 90° power divider with zig-zag-shaped slot for wireless communication applications," *Wirel. Pers. Commun.*, vol. 84, no. 4, pp. 2599-2611, Oct. 2015.
- [15] M. Winebrand and R. Vladimir, "Slot spiral miniaturized antenna," *United States Patent*, US6791497 B2, pp. 1-17, 2014.



Norhudah Seman received the B.Eng. in Electrical Engineering (Telecommunications) degree from the Universiti Teknologi Malaysia, Johor, Malaysia, in 2003 and M.Eng. degree in RF/Microwave Communications from The University of Queensland, Brisbane, St. Lucia, Qld., Australia, in 2005. In 2010, she received her Ph.D. degree from The University of Queensland. Currently, she is an Associate Professor and Director (Communication Engineering) in School of Electrical Engineering and Research Fellow in HiCoE Wireless Communication Centre (WCC), Universiti Teknologi Malaysia. Her research interests concern the design of microwave/millimeterwave devices for biomedical and industrial applications, effects of electromagnetic field radiation including specific absorption rate (SAR), and mobile communications.



Khairul Huda Yusof received the diploma in Electrical Engineering (Telecommunication) and degree of B.Eng. in Electrical Engineering (Microelectronics) from Universiti Teknologi Malaysia in 2008 and 2011, respectively. Currently, she just completed her Ph.D. study in

Electrical Engineering at Universiti Teknologi Malaysia, majoring in Telecommunication and has been appointed as a Lecturer in MAHSA University.



Mohd Haizal Jamaluddin was born in Selangor, Malaysia. He received his Bachelor degree and Master degree in Electrical Engineering from Universiti Teknologi Malaysia (UTM), Malaysia in 2003 and 2006, respectively. He received the Doctoral degree in Signal Processing and Telecommunications from the University of Rennes 1, Rennes, France in 2010. He is currently an Associate Professor UTM. His main field of interest is on antenna design, especially on dielectric resonator antenna, reflect array antenna and lens antenna.



Tharek Abd Rahman is a Professor at School of Electrical Engineering, Universiti Teknologi Malaysia (UTM). He obtained his B.Sc. in Electrical & Electronic Engineering from University of Strathclyde UK in 1979, M.Sc. in Communication Engineering from UMIST Manchester UK and Ph.D. in Mobile Radio Communication Engineering from University of Bristol, UK in 1988. He is the Director of Wireless Communication Centre (WCC), UTM. His research interests are radio propagation, antenna and RF design and indoors and outdoors' wireless communication. He has also conducted various short courses related to mobile and satellite communication to the Telecommunication Industry and Government body since 1990. He has a teaching experience in the area of mobile radio, wireless communication system and satellite communication.